Electronic Supplementary Material (ESI) for Metallomics.

Supporting Information

for

Arene ruthenium(II) complex, a potent inhibitor against prolification, migration and invasion of breast cancer that reduces stress fibers, focal adhension and invadopodia

CONTENTS

1. Experimental Section

1.1 Cell lines and cell culture

The human breast cancer high-metastastic MDA-MB-231 cells, and human normal kidney cells HK-2 and human skin immortalized epiderm cell line HaCat were purchased from American Type Culture Collection (ATCC, Manassas, VA). All cell lines were maintained in DMEM medium supplemented with fetal bovine serum (10%), penicillin (100 units/ml) and streptomycin (50 units/ml) at 37℃ in CO_2 incubator (95% relative humidity, 5% CO_2).

1.2 RT-qPCR analysis

Total RNA was isolated using Trizol (Invitrogen) according to the manufacture's recommendation. 2 μg of total RNA from each samples were reverse transcribed using oligo (dT) primers at 37°C for 90 min. The relative mRNA levels were evaluated by quantitative PCR using SYBR green PCR kit (Takara). The signals were normalized to 18 S as internal control. The quantity of miR-21 in each BC relative to the average expression in 40 NATs was calculated using the equation $RQ = 2^{-\Delta\Delta CT}$, where $\Delta\Delta C_T = (C_{T\ \mathrm{miRNA}} - C_{T\ \mathrm{U6\ RNA}})_S - (C_{T\ \mathrm{miRNA}} - C_{T\ \mathrm{U6\ RNA}})\mathrm{Mean}_C$. The primers were as follows:

PTEN Forward, 5'-CGACGGGAAGACAAGTTCAT-3'

Reverse, 5'-AGGTTTCCTCTGGTCCTGGT-3'

AKT Forward, 5'-ACAAGGACGGGCACATTAAG-3'

Reverse, 5'-GTCATTGTCCTCCAGCACCT-3'

Gsk3β Forward, 5'-AAAGGTGATTCGCGAAGAGA-3'

Reverse, 5'-CCACCACTGTTGTCACCTTG-3'

p21 Forward, 5'-TGTCCGTCAGAACCCATGC-3'

Reverse, 5'-AAAGTCGAAGTTCCATCGCTC-3'

MMP-2 Forward, 5'-CCCACTGCGGTTTTCTCGAAT-3'

Reverse, 5'-CAAAGGGGTATCCATCGCCAT-3'

MMP-9 Forward, 5'-GGGACGCAGACATCGTCATC-3'

Reverse, 5’-TCGTCATCGTCGAAATGGGC-3’

18S Forward, 5’-AACCCGTTGAACCCCATT-3’

Reverse, 5’-CCATCCAATCGGTAGTAGCG-3’)

miR-21,UAGCUUAUCAGACUGAUGUUGA

U6 Forward, 5’GTGCTCGCTTCGGCAGCACATATAC

Reverse, 5’ AAAAATATGGAACGCTTCACGAATTTG

2. RESULTS

2.1 Synthesis and characterization

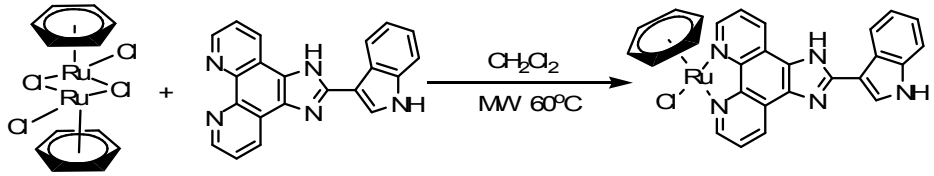

Figure S1 The synthetic route of [(η^6-C_6H_6)Ru(H_2iip)Cl]Cl

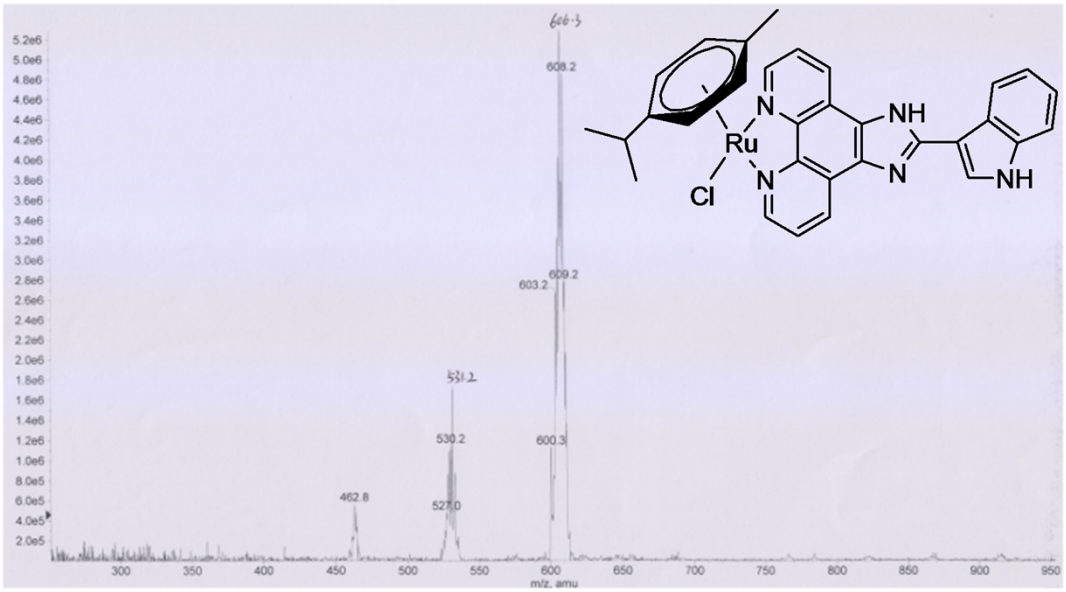

Figure S2 The ESI-MS spectrum of arene Ruthenium complex **1**

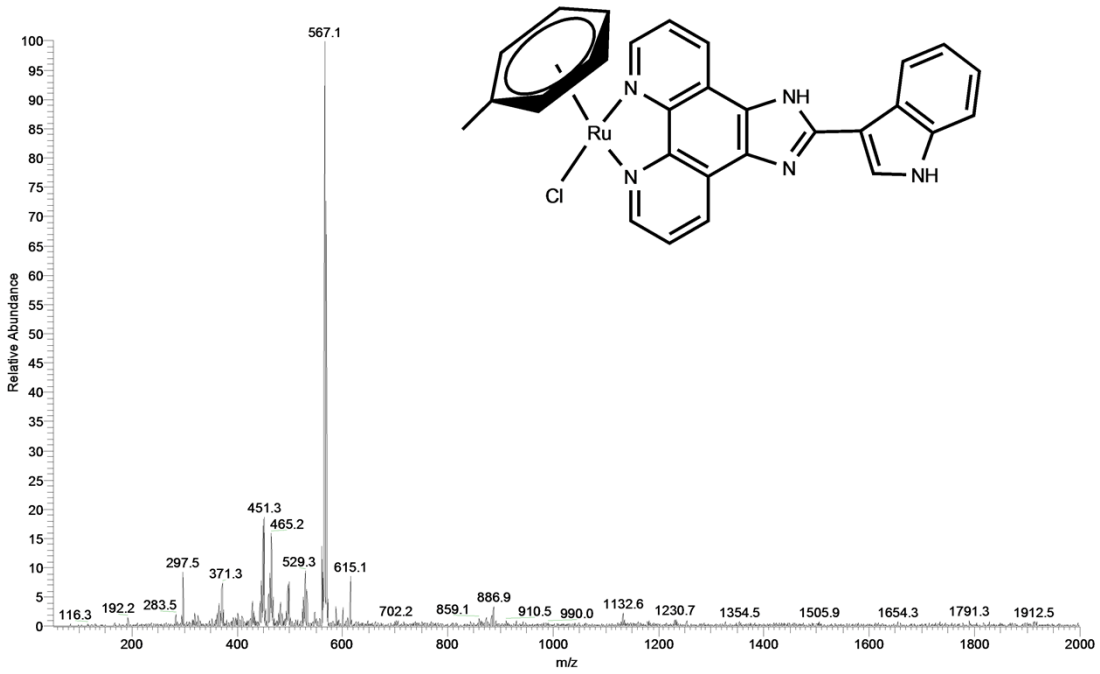

Figure S3 The ESI-MS spectrum of arene Ruthenium complex **2**

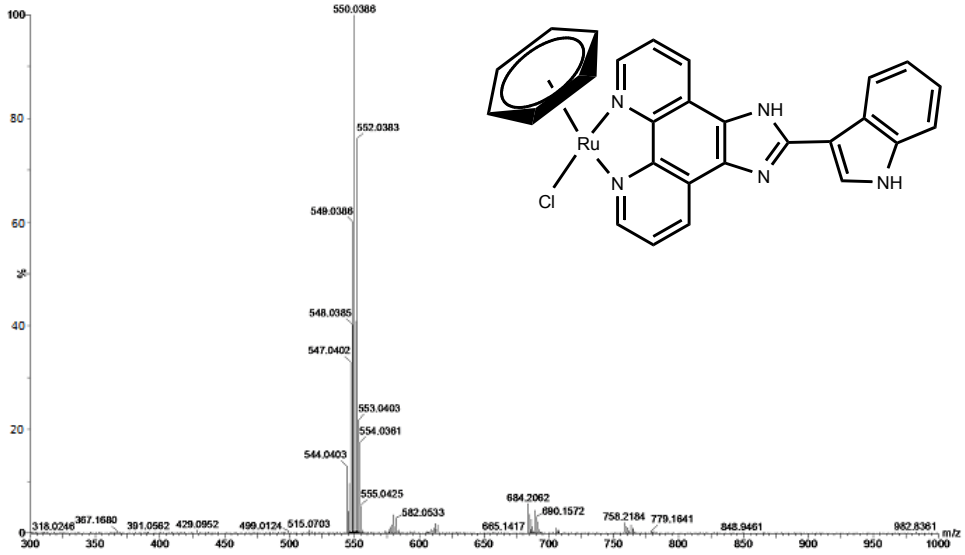

Figure S4 The ESI-MS spectrum of arene Ruthenium complex **RAWQ11**

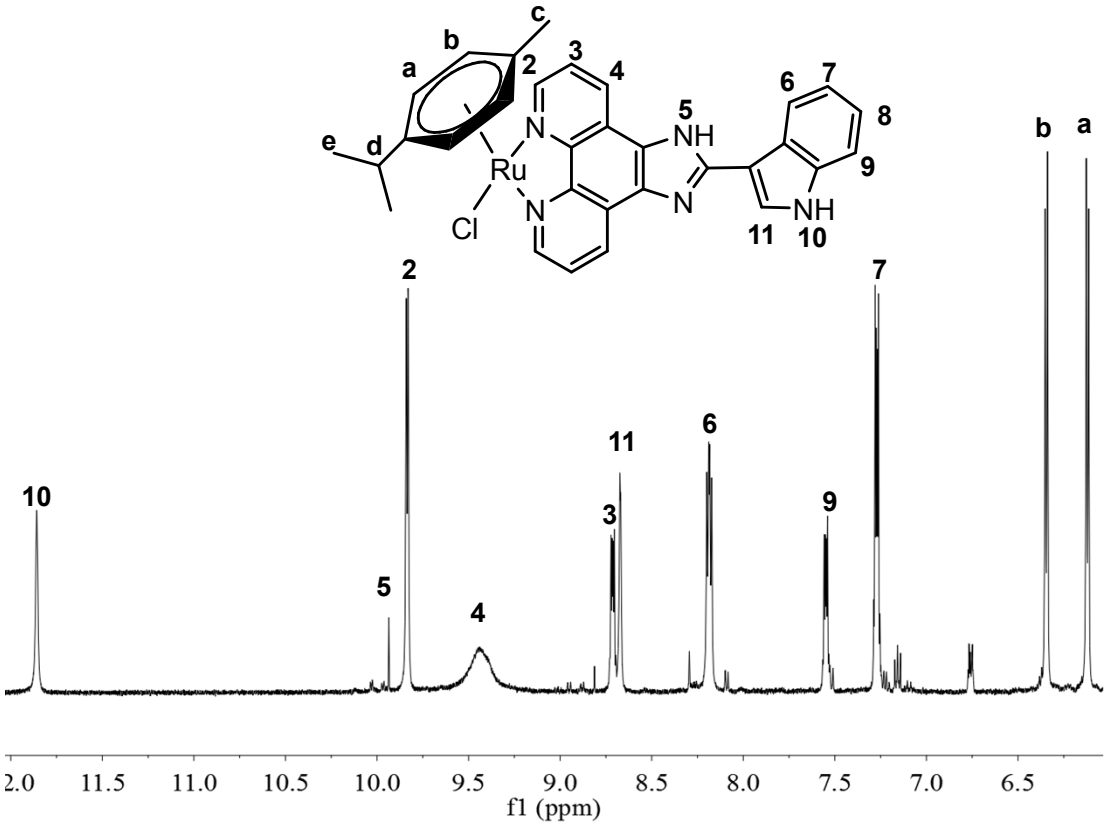

Figure S5 The **^{1}H NMR spectrum of arene Ruthenium complex 1**

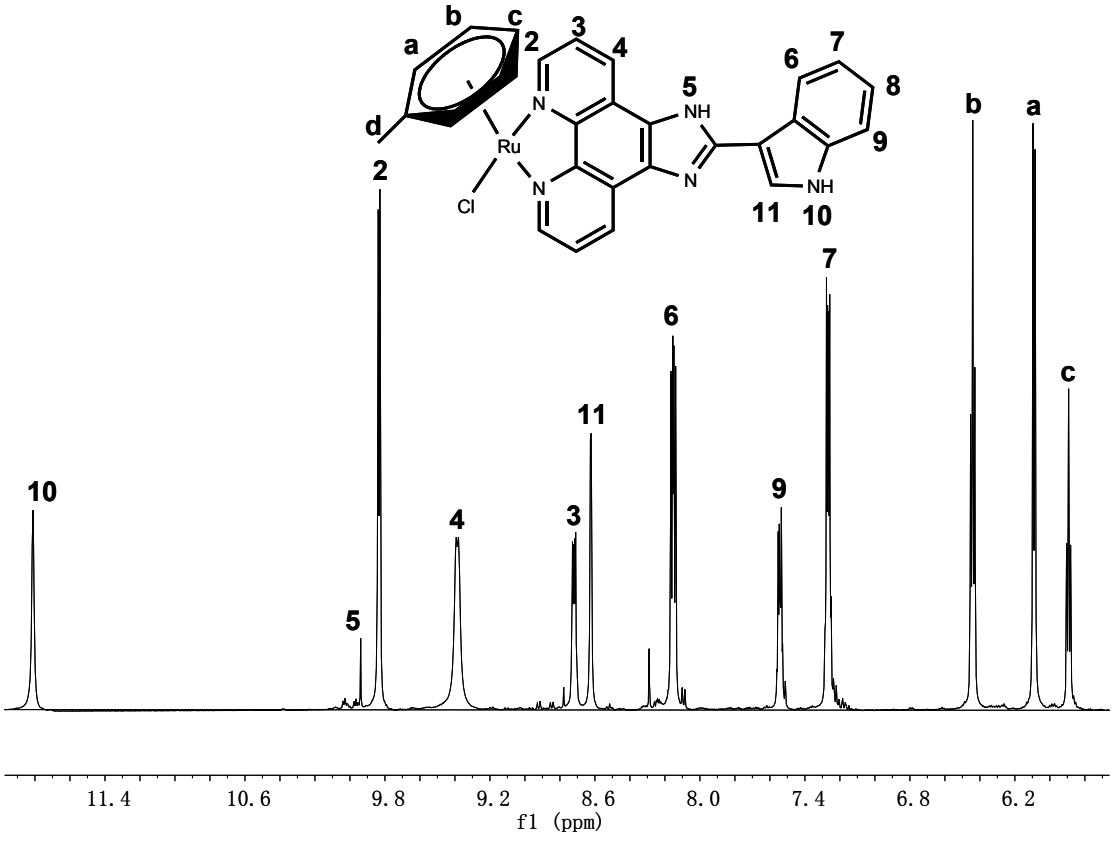

Figure S6 The **^{1}H NMR spectrum of arene Ruthenium complex 2**

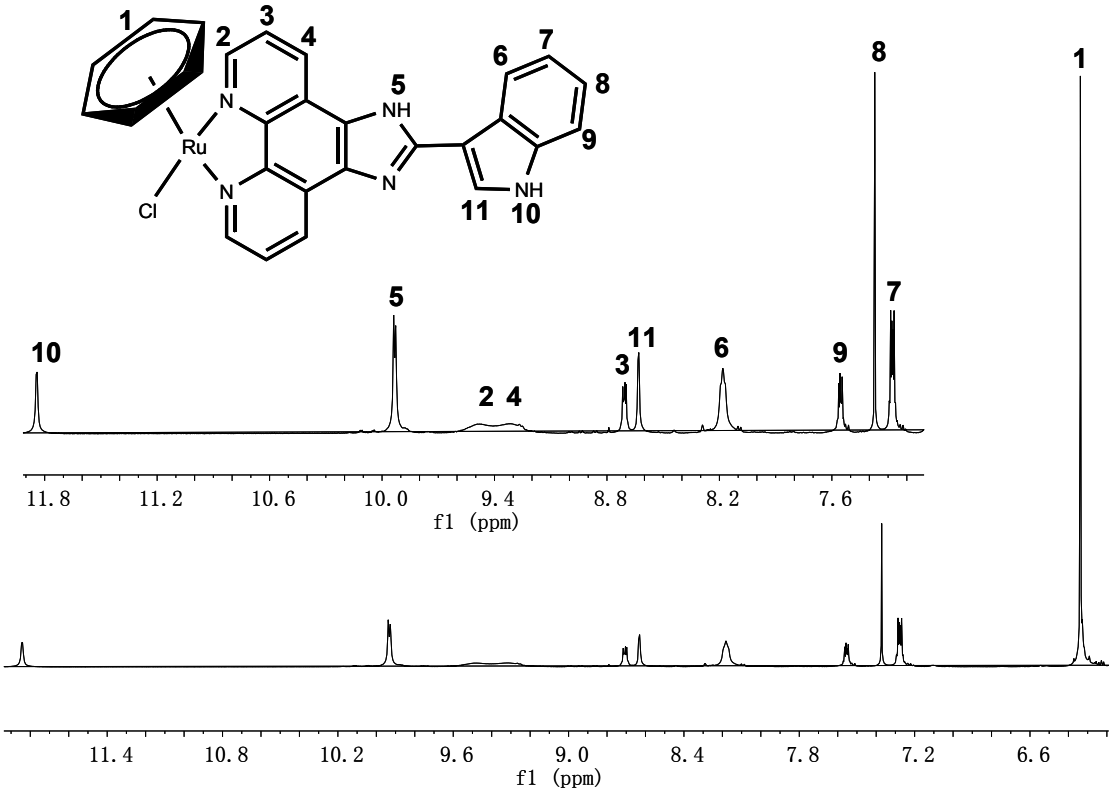

Figure S7 The **^{1}H NMR spectrum of arene Ruthenium complex 3**

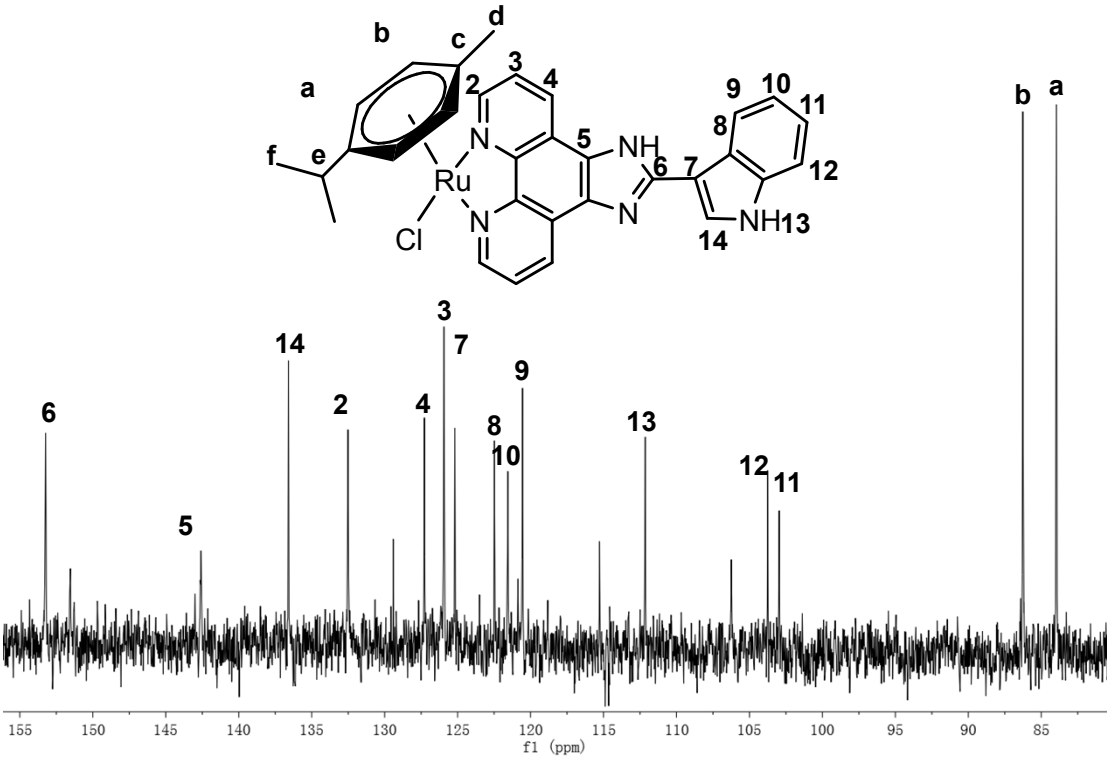

Figure S8 The ^{13}C NMR spectrum of arene Ruthenium complex **RAWQ03**

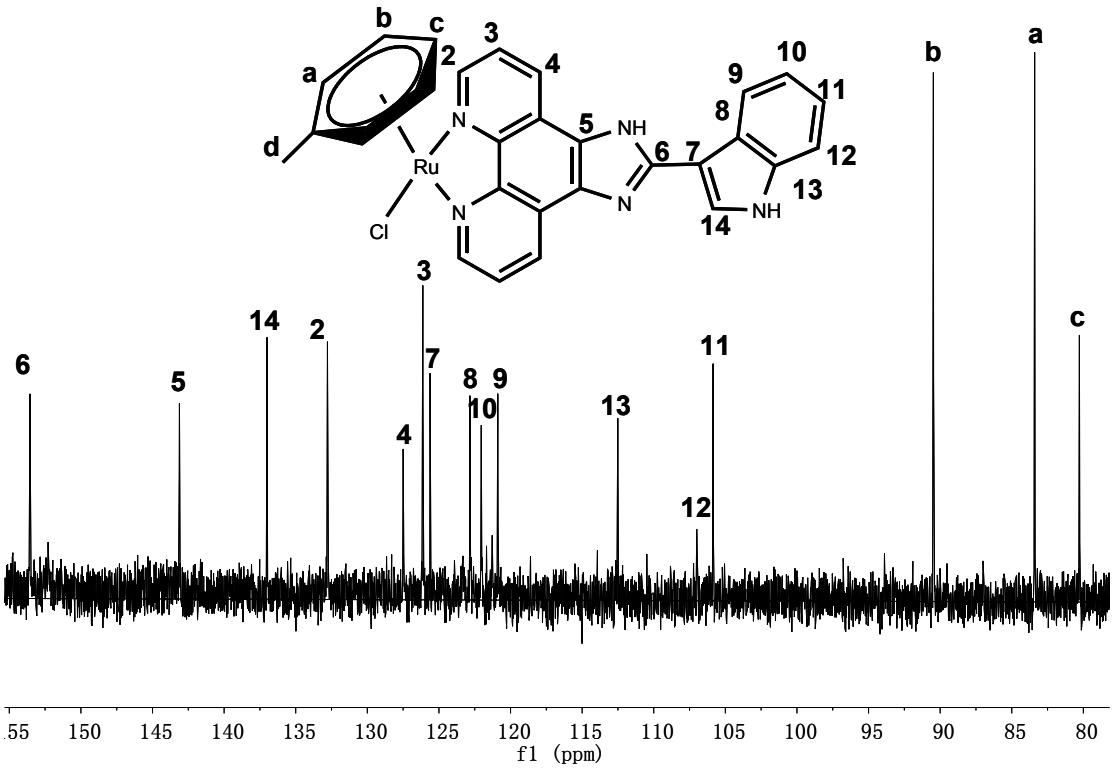

Figure S9 The ^{13}C NMR spectrum of arene Ruthenium complex **RAWQ04**

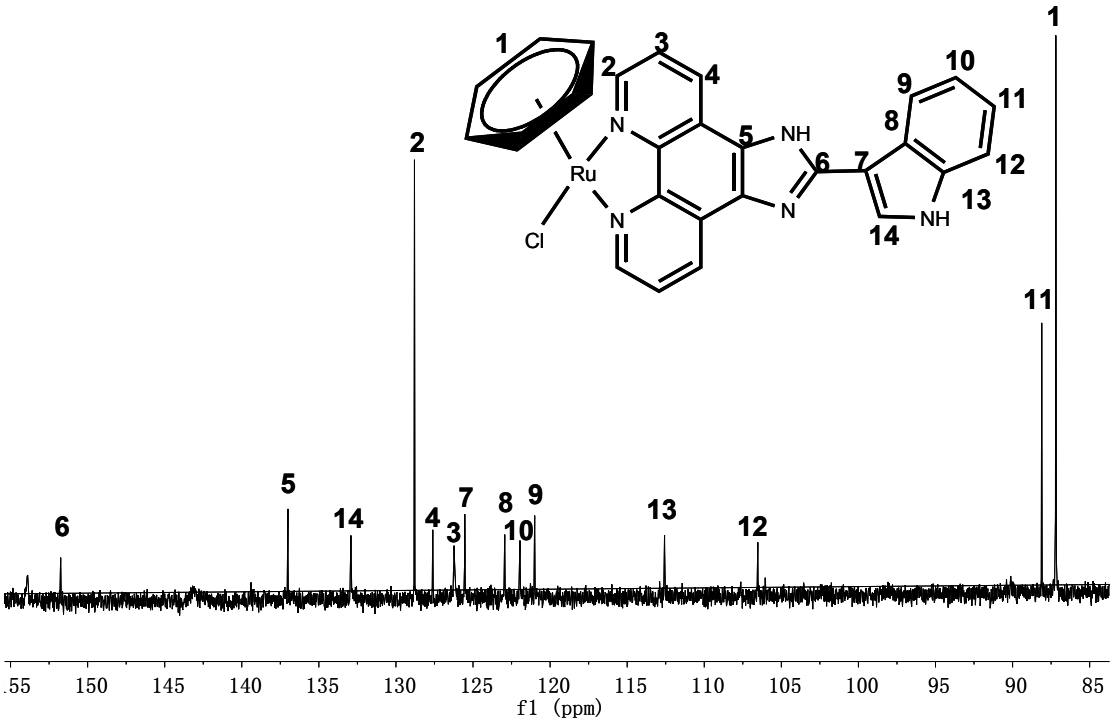

Figure S10 The ^{13}C NMR spectrum of arene Ruthenium complex **RAWQ11**

2.2 Crystal data of 3

Table S1 Crystal data and structure refinement for **RAWQ11**

Empirical formula	$C_{27}H_{18}N_5ClO_{2.25}Ru$
Formula weight	554
Temperature/K	297
Crystal system	tetragonal
Space group	$P\text{-}42_1c$
a/Å	27.1414(5)
b/Å	27.1414(5)
c/Å	7.5825(4)
α/°	90
β/°	90
γ/°	90
Volume/Å^3	5585.7(3)
Z	8
ρ_{calc}mg/mm^3	1.3175
m/mm^{-1}	0.68
F(000)	2223.9
2Θ range for data collection	6 to 50°
Index ranges	$-36 \le h \le 34$, $-37 \le k \le 19$, $-9 \le l \le 10$
Reflections collected	18947
Independent reflections	4856[R(int) = 0.0756]
Data/restraints/parameters	4856/6/308
Goodness-of-fit on F^2	1.648
Final R indexes [I>=2σ (I)]	R_1 = 0.0979, wR_2 = N/A
Final R indexes [all data]	R_1 = 0.1180, wR_2 = 0.3053
Largest diff. peak/hole / e Å^{-3}	3.81/-0.74
Flack parameter	-0.08(13)

Table S2 Bond Lengths for **RAWQ11**

Atom	Atom	Length/Å	Atom	Atom	Length/Å
Ru1	Cl1	2.396(4)	N3	C12	1.431(19)
Ru1	N1	2.086(11)	N3	C13	1.40(2)
Ru1	N2	2.059(13)	C8	C7	1.42(2)
N1	C1	1.373(18)	C17	C18	1.39(2)
N1	C5	1.357(17)	C17	C22	1.29(2)
N5	C17	1.45(2)	C6	C5	1.40(2)
N5	C16	1.39(2)	C6	C10	1.41(2)
C3	C2	1.37(2)	C18	C14	1.51(2)
C3	C4	1.436(19)	C18	C19	1.37(2)
C1	C2	1.411(19)	C16	C14	1.36(2)
N4	C11	1.404(19)	C13	C14	1.41(2)
N4	C13	1.29(2)	C22	C21	1.35(3)
C11	C12	1.39(2)	C19	C20	1.29(2)
C11	C10	1.44(2)	C21	C20	1.54(3)
N2	C6	1.446(18)	C28	C23	1.377(9)
N2	C7	1.36(2)	C28	C27	1.382(9)
C4	C12	1.404(19)	C23	C24	1.388(9)
C4	C5	1.387(19)	C25	C24	1.380(9)
C9	C8	1.38(2)	C25	C26	1.385(9)
C9	C10	1.41(2)	C27	C26	1.383(9)

Table S3 Bond Angles for **RAWQ11**

Atom	Atom	Atom	Angle/°	Atom	Atom	Atom	Angle/°
N1	Ru1	Cl1	84.7(4)	C10	C6	N2	119.5(13)
N2	Ru1	Cl1	84.7(4)	C10	C6	C5	124.9(13)
N2	Ru1	N1	78.4(5)	C14	C18	C17	106.9(13)
C1	N1	Ru1	125.4(9)	C19	C18	C17	117.5(15)
C5	N1	Ru1	116.2(9)	C19	C18	C14	135.4(14)
C5	N1	C1	118.4(11)	C4	C5	N1	123.7(12)
C16	N5	C17	108.7(13)	C6	C5	N1	115.9(12)
C4	C3	C2	120.5(12)	C6	C5	C4	120.3(12)
C2	C1	N1	121.5(13)	C14	C16	N5	110.3(14)
C13	N4	C11	110.4(13)	C8	C7	N2	122.3(15)
C12	C11	N4	104.6(13)	C9	C10	C11	127.4(15)
C10	C11	N4	132.2(15)	C6	C10	C11	112.5(13)
C10	C11	C12	123.2(15)	C6	C10	C9	120.1(14)
C1	C2	C3	118.5(14)	N3	C13	N4	112.3(13)
C6	N2	Ru1	113.8(9)	C14	C13	N4	124.8(16)
C7	N2	Ru1	127.9(12)	C14	C13	N3	122.4(13)
C7	N2	C6	118.1(14)	C16	C14	C18	106.8(12)
C12	C4	C3	125.8(13)	C13	C14	C18	127.7(13)
C5	C4	C3	116.7(12)	C13	C14	C16	125.5(15)
C5	C4	C12	117.4(12)	C21	C22	C17	122.0(18)
C10	C9	C8	119.8(15)	C20	C19	C18	121.2(17)
C13	N3	C12	102.4(12)	C20	C21	C22	114.3(16)
C4	C12	C11	121.7(13)	C21	C20	C19	120.3(18)
N3	C12	C11	110.2(13)	C27	C28	C23	124.0(17)
N3	C12	C4	128.0(14)	C24	C23	C28	113.7(16)
C7	C8	C9	119.7(15)	C26	C25	C24	111.6(17)
C18	C17	N5	107.2(13)	C26	C27	C28	116.0(17)
C22	C17	N5	128.6(16)	C25	C24	C23	128.5(18)
C22	C17	C18	124.2(17)	C27	C26	C25	126.0(18)
C5	C6	N2	115.5(14)				

2.2 MTT assay

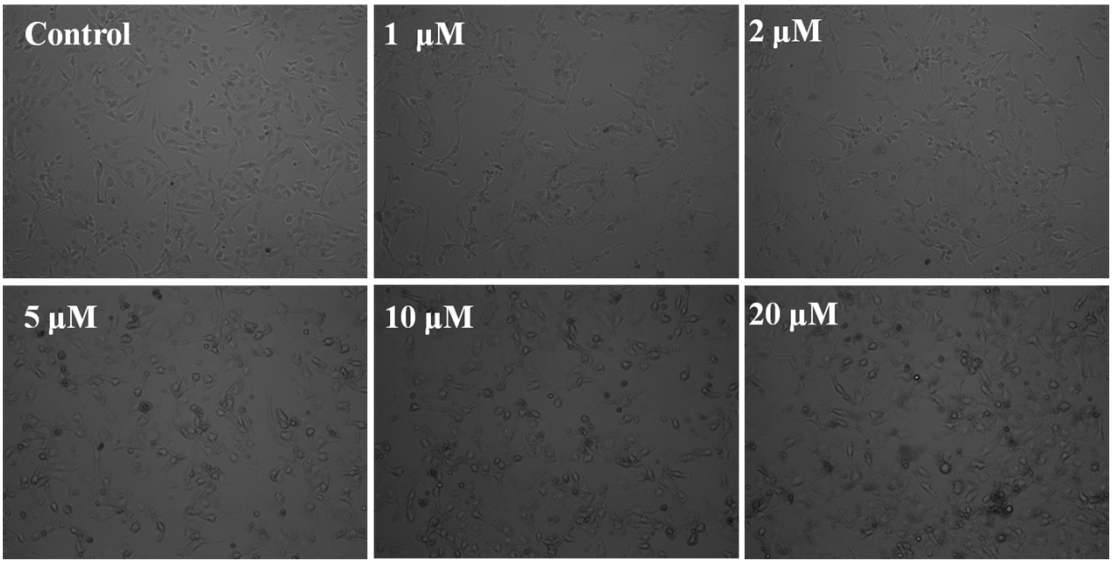

Figure S11 *In vitro* anticancer activity of complex **RAWQ11** against MDA-MB-231 cells.

2.3 Wound healing assay

A

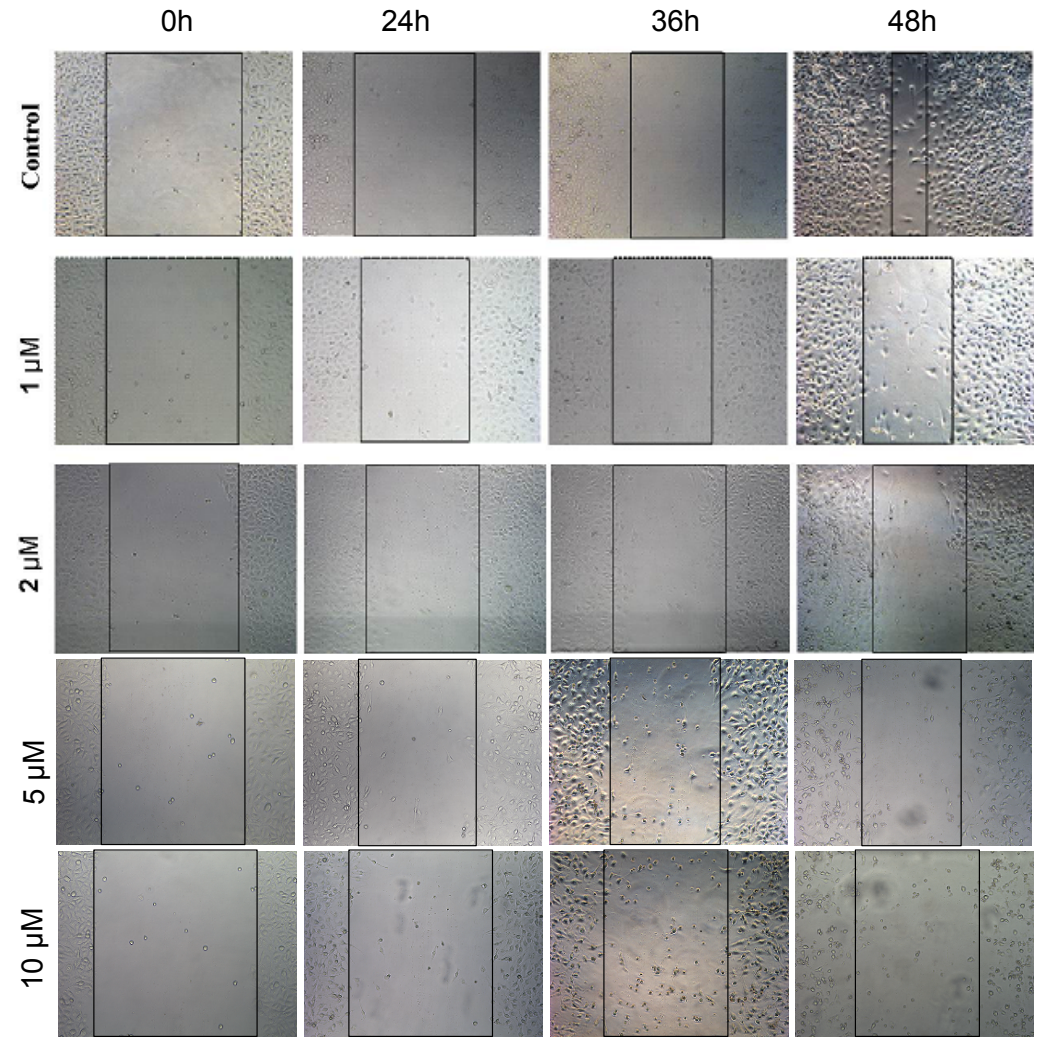

B

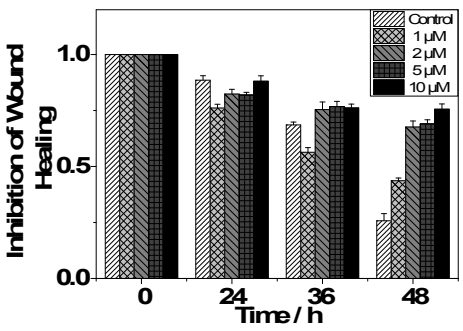

C

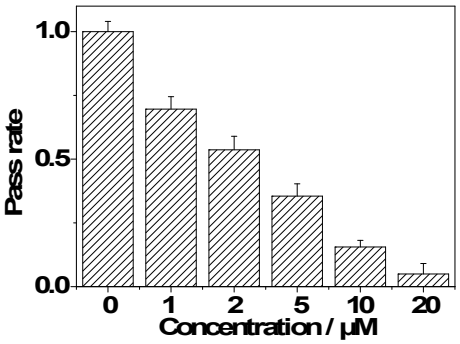

Figure S12 (**A**)The wound healing assay was used to evaluate the migration of MDA-MB-231 cells after dealted with **RAWQ11** (0, 1, 2, 5 and 10 μM), DMEM with 10% FBS. Cells were

wounded and monitored with a microscope every 12 hours. The migration was determined by the rate of cells filling the scratched area. (**B**) The wound distance decreased rate following the increasing of time by treated with **RAWQ11** (0, 1, 2, 5 and 10 μM). (**C**) The rate of MDA-MB-231 cells invaded matrigel to the other side of membrane when treated with **RAWQ11** (0, 1, 2, 5, 10 and 20 μM) for 24 h in transwell assay.

2.4 FITC-gelatin assay

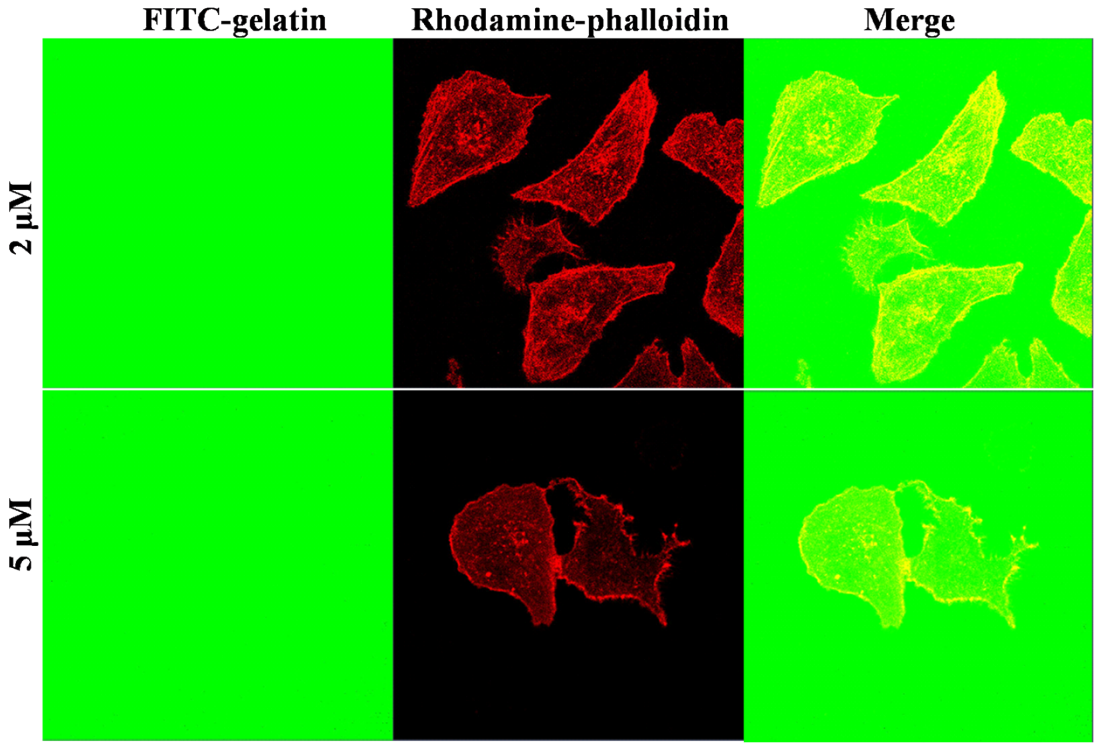

Figure S13 Immunofluorescent localization of F-actin of MDA-MB-231 cells treatment with **RAWQ11** (2 and 5 μM) for 24 h. Following the increase of **RAWQ11**, the number of cells decreased, cell polarity lost, F-actin depolymerized and the black hole in FITC-gelatin reduced.

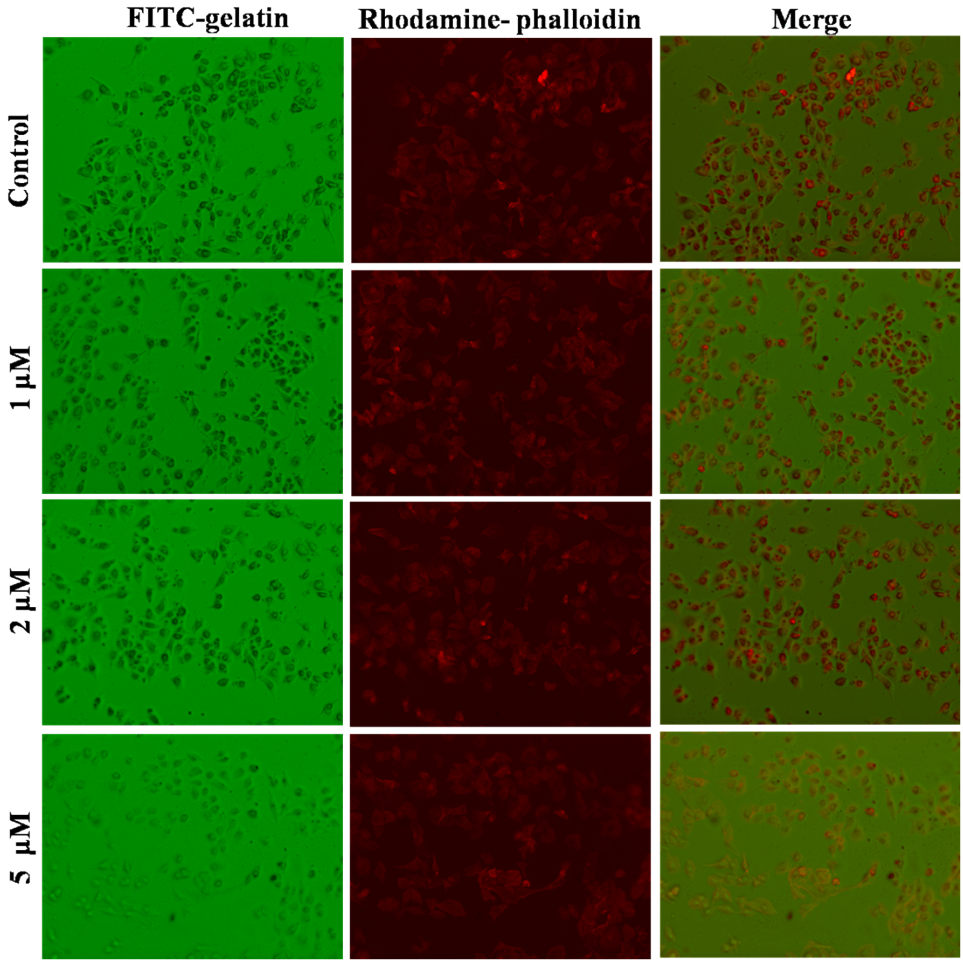

Figure S14 Immunofluorescent localization of F-actin of MDA-MB-231 cells treatment with **NAMI-A** (0, 1, 2 and 5 μM) for 24 h. Following the increase of **NAMI-A**, the number of cells decreased, F-actin depolymerized and the black hole in FITC-gelatin reduced.